ISSN 0023-1584, Kinetics and Catalysis, 2009, Vol. 50, No. 1, pp. 57–64. © Pleiades Publishing, Ltd., 2009.
Original Russian Text © M.N. Timofeeva, S.Ts. Khankhasaeva, 2009, published in Kinetika i Kataliz, 2009, Vol. 50, No. 1, pp. 63–71.

FIFTY YEARS
OF THE BORESKOV INSTITUTE OF CATALYSIS

Regulating the Physicochemical and Catalytic Properties of Layered Aluminosilicates

M. N. Timofeeva[a] and S. Ts. Khankhasaeva[b]

[a] *Boreskov Institute of Catalysis, Siberian Branch, Russian Academy of Sciences, Novosibirsk, 630090 Russia*
[b] *Baikal Institute of Nature Management, Siberian Branch, Russian Academy of Sciences, Ulan-Ude, 670047 Russia*
e-mail: timofeeva@catalysis.ru, shan@binm.bscnet.ru

Received February 27, 2008

Abstract—Basic methods of the introduction of metal ions into the interlayer space of natural layered aluminosilicate (LAS) are considered. The physicochemical and structural properties of pillared LAS's depend on the nature of the cation, as well as on the cation intercalation method and conditions. The catalytic properties and stability of an LAS in acid-catalyzed and oxidation reactions may depend on its textural and physicochemical properties.

DOI: 10.1134/S002315840901008X

At present, considerable attention is focused on the development of new, environmentally friendly and functionally active sorbents, supports, and catalysts based on layered aluminosilicates (LAS's) [1–6]. In the early 1970s, new types of catalysts based on layered silicates were created, which received the names of pillared sheet silicates and cross-linked or fixed-layer silicates [6]. Only limited information about these systems is available from the Russian literature. The interest in these materials is due to their unique physicochemical and textural properties, such as large specific surface area, thermal stability, and fairly large interlayer spacing (14–20 Å). As a rule, the textural and physicochemical properties of these materials depend on many parameters, including the chemical composition of the initial LAS, the nature of the M^{n+} cation introduced into the interlayer space, the $OH^-/(Al^{3+} + M^{n+})$ ratio, the way in which the cation was introduced, and the LAS calcination temperature. From the standpoint of acid catalysis, of great interest is the fact that the acidic properties of an LAS can be regulated by varying the nature of the intercalated cation [1, 7]. The introduction of transition metal ions capable of undergoing reversible redox conversions opens up great application opportunities for modified LAS's as redox catalysts [1–6]. Note that use of mixed oligomeric cations, e.g., Al–Ti, Al–La, and Al–Ce, has made it possible to obtain functional catalytic systems that can accelerate redox process and possess high surface acidity [1].

Although these systems have been studied extensively by both Russian and foreign researchers, there is, unfortunately, no consensus as to the effect of modification (pillaring) on the structural, physicochemical, and catalytic properties of LAS's. Here, we will summarize the results of our studies of the influence of the most important pillaring parameters, such as the nature of the cation, pillaring procedure, and the formation temperature of the layered pillared structure (LAS calcination temperature), on the textural and physicochemical properties of the resulting materials [8–14]. The widest application has been found by pure montmorillonite clays, or bentonites. For this reason, we used clay from the Mukhortalinskoe deposit (Buryat Republic). Our main focus will be placed on the correlation between the clay modification methods, the textural and physicochemical properties of modified clays, and the catalytic properties of these clays in acid-catalyzed and oxidation reactions.

TEXTURAL AND PHYSICOCHEMICAL PROPERTIES OF LAS'S

Effect of the Nature of the Cation Introduced into the Interlayer Space on the Textural and Physicochemical Properties of the LAS

A possible way of regulating the textural and physicochemical properties of an LAS is by modifying its structure by exchanging its cations for voluminous polynuclear hydroxo cations of Al^{3+}, Fe^{3+}, Ti^{4+}, Zr^{4+}, etc. Upon heating, the complex cations turn into their respective metal oxides, which act as pillars to fix the silicate layers at a certain distance from one another, thereby producing regular porous structures (Fig. 1) [15, 16]. Modifying LAS's by this method enhances their specific surface area, microporosity, and thermal stability—parameters significant to sorbent and catalytic applications of these clays. Table 1 lists the most important textural and physicochemical properties of LAS's prepared by introducing Na^+ and H_3O^+ cations and the large polynuclear cation $[Al_{13}O_4(OH)_{24}(H_2O)_{12}]^{7+}$ into the interlayer space. As is

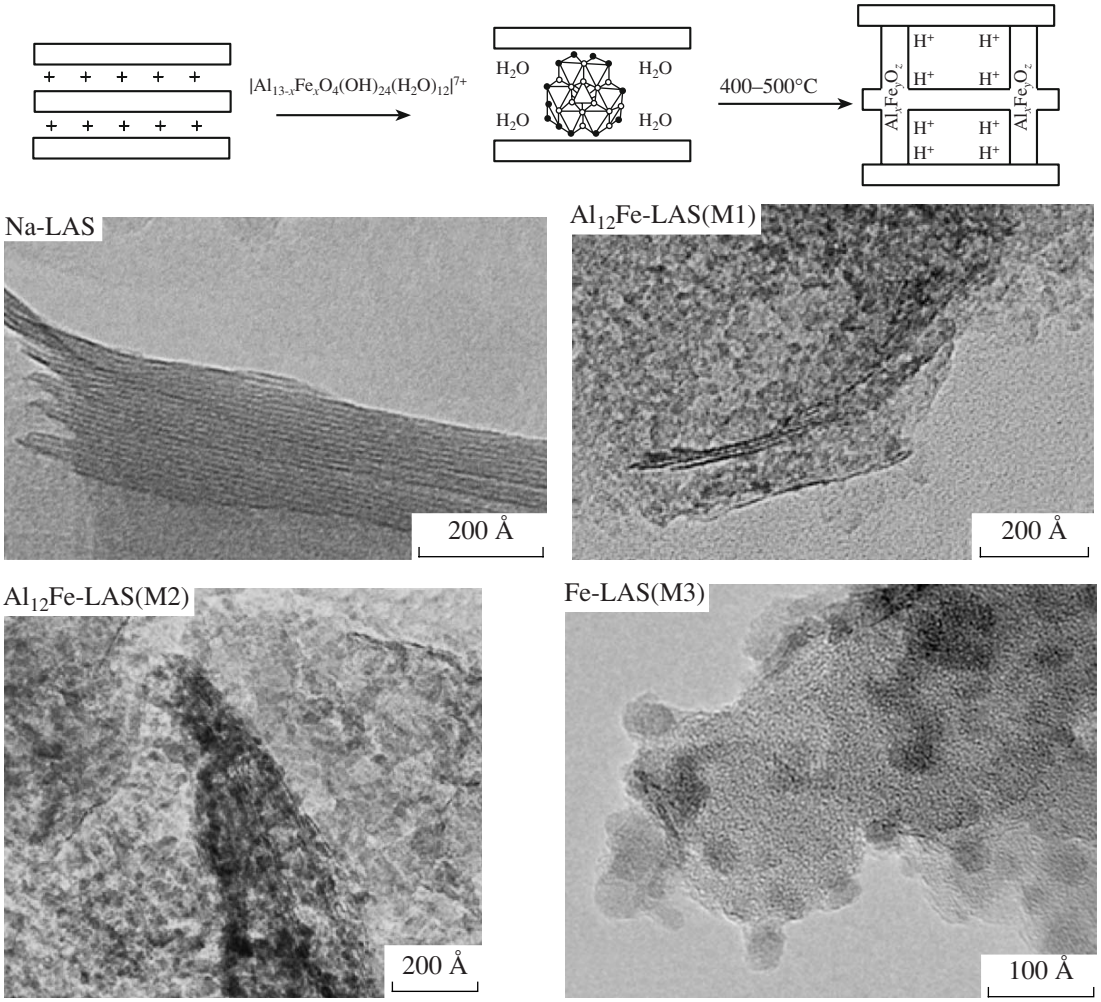

Fig. 1. Intercalation of the polynuclear cation $[Al_{13-x}Fe_xO_4(OH)_{24}(H_2O)_{12}]$ into Na-LAS and electron micrographs of various LAS's.

clear from Table 1, the textural parameters of the modified clays depend significantly on the nature of the intercalated cation. For example, the mean pore diameter increases in the order Al_{13}-LAS < Na-LAS < natural LAS. As compared to natural LAS, H-LAS, and Na-LAS, Al_{13}-LAS has a much larger number of micropores 8–9 Å in diameter, whose surface area can be as large as 33–56 m^2/g.

The strongest dependence on the nature of the intercalated cation is shown by the acidic properties of the LAS's. By nonaqueous titration with *n*-butylamine in the presence of Hammett indicators [8], it was established that modification of LAS with H_3O^+ ions (1 M HCl) and $[Al_{13}O_4(OH)_{24}(H_2O)_{12}]^{7+}$ ions significantly increases the amount of sites with a strength of $H_0 < -3.0$ (Table 1). The appearance of acid sites with $H_0 = -5.6$ in Na-LAS after calcination at 500°C indicates that the hydroxylation temperature is a crucially significant factor in the formation of strong acid sites. The strong polarization of the OH bonds in the adsorbed water molecules favors the appearance of mobile protons in the oppositely charged fields of the surface oxygen atoms and exchanged cations:

$$M^{3+} + nH_2O \rightleftharpoons [M(OH)_n]^+ + nH^+.$$

The degree of dissociation increases as the polarizing power of the cation increases in the order $Na^+ < Mg^{2+} < Al^{3+}$ [6].

In the presence of a large amount of water, the polarization effect arising from the interaction between the cation and water is weaker. According to Tarasevich et al. [7, 17], the appearance of sites with $H_0 = -5.6$ is due to the presence of exchanged Al^{3+} cations and coordinatively unsaturated Al^{3+} cations in the environment of three structural oxygen atoms. The existence of $AlO_4\square_2$ ($\square$ = vacancy) sites on the LAS surface is responsible for the formation of sites with $H_0 = -3.0$; the presence of polarized Si–OH* groups, for the formation of sites with $-3.0 < H_0 \le 1.5$ [7, 18]. The LAS's containing 0.5–1.0% water have mainly Brønsted acidity. As the water content of H-LAS, Na-LAS, and Al_{13}-LAS is decreased, the strength of their acid sites increases

Table 1. The most important physicochemical and catalytic properties of LAS's

Material	Calcination temperature, °C	Textural characteristics				$k \times 10^4$, s^{-1}	Acid site content, mol/g					*L*/*B*
		S_{BET}, m^2/g	S_μ, m^2/g	D_{por}, Å	d_{100}, Å		$H_o = -5.6$	$H_o = -3.0$	$H_o = +3.3$	$H_o = +4.8$	*L*	
Natural clay	500	109	–	93	11	0	–	–	–	–	–	–
	400	144	–	82	14	0.1	–	0.02	0.18	0.32	–	–
Na-LAS	500	141	–	84	15	2.1	0.01	0.04	0.30	0.42	0.03	0.08
	400	–	–	–	–	1.8	0.08	0.13	0.20	0.25	–	–
H-LAS	500	–	–	–	–	4.7	0.10	0.20	0.28	0.41	0.04	0.11
	400	203	56	65	18	3.5	–	–	–	–	–	–
Al_{13}-LAS	500	179	33	68	18	9.3	0.10	0.24	0.32	0.43	0.06	0.16

Note: S_μ is the specific surface area of the pores, D_{por} is the mean pore diameter, d_{100} is the interlayer spacing (X-ray diffraction data), k is the acetone dimerization rate constant (50°C, catalyst content of 10 wt %), *L* is the total amount of Lewis sites determined by IR spectroscopy using CO adsorption, and *L*/*B* is the molar ratio of the Lewis sites to the Brønsted sites. The amounts of acid sites of different strengths (H_0) were determined by nonaqueous titration with *n*-butylamine in the presence of an indicator.

(Table 1) and Lewis acid sites appear. For example, the replacement of some tetravalent silicon with Al^{3+} in the tetrahedral networks, raising the proportion of tetrahedrally coordinated aluminum, shifts the absorption bands at 1090 and 1044 cm^{-1} in the IR spectrum of Al_{13}-LAS, which are due to stretching vibrations of silicon–oxygen tetrahedra, to lower frequencies (Fig. 2a). This indicates an increase in the mean (Si,Al)–O distance and in the ionicity of the corresponding band [7, 17, 18]. The increasing separation of silicate layers and the enhancement of the ionicity of the matrix generate strong Lewis sites (Table 1). Note, however, that the introduction of the $[Al_{13}O_4(OH)_{24}(H_2O)_{12}]^{7+}$ cation into the LAS structure raises the total amount of sites only slightly over the amount of sites in the acid form H-LAS. Therefore, the aluminum cations in the Al_{13}-LAS system are distributed randomly and not all of them are accessible to *n*-butylamine molecules. This is also indicated by low-temperature CO adsorption data [8]. According to these data, Al_{13}-LAS has several types of Lewis sites, which show themselves as absorption bands at 2229 and 2195–2185 cm^{-1} (Fig. 2b). The latter is also observed for CO adsorbed on alumina [19]. The presence of acidic OH groups is indicated by absorption bands in the 2175–2160 cm^{-1} range. The strong absorption band at 2167 cm^{-1} is due to weak H-complexes of CO with the Si–OH group (characterized by an absorption band at 3745 cm^{-1}). In addition, the spectrum in the region of OH group vibrations exhibits a band at 3660 cm^{-1}, which is due to the polarized inter-

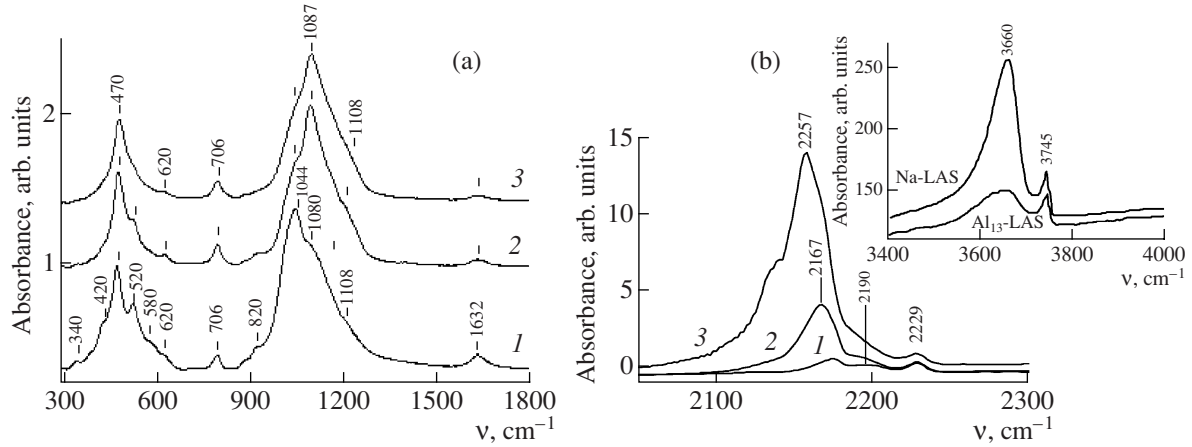

Fig. 2. (a) IR spectra of (*1*) natural LAS, (*2*) Na-LAS, and (*3*) Al_{13}-LAS. (b) IR spectra of CO adsorbed on Al_{13}-LAS at pressures of (*1*) 0.1, (*2*) 0.9, and (*3*) 10 Torr. Inset: IR spectra of the hydroxyl groups of (*1*) Na-LAS and (*2*) Al_{13}-LAS after vacuum pumping at 450°C.

Table 2. Dependence of the textural and catalytic properties of LAS's in phenol oxidation with hydrogen peroxide on the way of introducing iron ions into the interlayer space

Sample no.	Material	Method	Textural characteristics			Fe content, mg/g	Time, min	PhOH conversion, %	Δ_{Fe}, wt %
			S_{BET}, m^2/g	V_Σ, cm^3/g	D_{por}, Å				
1	Natural clay	–	113	0.28	97	8 ± 2	420	0	–
2	Al_{13}-LAS	–	242	0.25	73	8 ± 2	420	0	–
3	$Al_{12}Fe$-LAS	M1	244	0.25	72	15 ± 2	105 (105)*	50	<0.01
							180 (180)*	100	
4	$Al_{6.5}Fe_{6.5}$-LAS	M1	136	0.24	64	32 ± 5	325	50	12
							420	100	
5	$Al_{12}Fe$-LAS	M2	203	–	–	21 ± 1	105 (180)*	50	19
							180 (320)*	100	
6	Fe-LAS(OH)	M3	136	0.27	76	28 ± 1	120	50	18
							270	100	
7	Fe-LAS(OH)	M3	132	0.27	76	11 ± 1	95	50	6
							110	100	
8	Fe-LAS(Cl)	M3	125	0.32	103	23 ± 1	95	50	18
							130	100	

Note: Reaction conditions: [PhOH] = 1 mmol/l; [H_2O_2] = 14 mmol/l; amount of catalyst, 1 g/l; pH 6.2; T = 50°C. OH/(Fe + Al) = 2.0 : 1. All samples were calcined at 400°C prior to the reaction. Δ_{Fe} is the amount of iron washed out into the solution during the reaction.

* The catalyst was reused.

layer OH* groups. These groups play an important role in the formation of the protonic acidity of the LAS. This band in the spectrum of Al_{13}-LAS is weaker than the same band in the spectrum of Na-LAS (Fig. 2b). This is likely explained by the fact that the OH* groups in these materials are in different structural environments, resulting in different capacities for CO adsorption. These data are in agreement with crystal chemical data for the lateral face of a dioctahedral layered silicate [6, 7], which indicate the presence of three types of acidic hydroxyl groups, namely, ordinary (Si–OH), polarized (Si–OH*), and bridging hydroxyls. Depending on the nature of the octahedrally coordinated cation, the acidity of ordinary and polarized Si–OH groups can vary in a wide range.

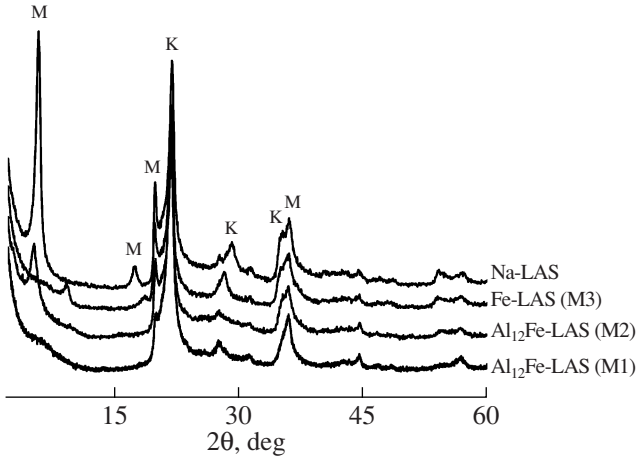

Fig. 3. X-ray diffraction patterns of the Na-LAS, Fe-LAS, and $Al_{12}Fe$-LAS systems prepared by different methods.

Influence of the Iron Ion Intercalation Method on the Textural Properties of LAS's

The introduction of iron ions as the polyhydroxo complex $Fe_x(OH)_y^{n+}$ or the mixed polynuclear cation affords materials with a basal spacing of up to 19 Å and a large specific surface area (up to 240 m^2/g) [20, 21]. The iron ions to be introduced into Na-LAS can be a component of the large polynuclear cation $[FeO_4Al_{12}(OH)_{24}(H_2O)_{12}]^{7+}$ (method M1). Iron in the form of $Fe_x(OH)_y^{n+}$ polyhydroxo complexes can be introduced into the interlayer space of Al_{13}-LAS and Na-LAS (methods M2 and M3, respectively). The following natural question arises here: Which of these methods will afford the system with the largest specific surface area, the highest microporosity, the highest degree of dispersion of the metal, and the highest resis-

tance to metal washout from the matrix? Table 2 lists the most important textural parameters of the materials obtained by these three methods [10, 14]. According to X-ray diffraction data, the intensity of the first basal reflection (d_{001}) depends on the LAS modification method (Fig. 3). The low intensity and diffuseness of the peaks at small 2θ angles in the diffraction patterns of Fe-LAS (M3) and Al_{12}Fe-LAS (M1) suggest that the layered structures of these materials have changed from the initial LAS structure more radically than the Al_{12}Fe-LAS (M2) structure, even though the specific surface areas of the samples prepared by the methods M1 and M2 differ insignificantly (Table 2). This is also indicated by electron microscopic data (Fig. 1). Na-LAS has a fibrous structure. The montmorillonite particles are platelike. Randomly distributed in space, they form secondary pores differing in shape and size. The introduction of bulky polynuclear cations into the interlayer space of the LAS markedly swells the material and, as a consequence, causes LAS separation. Upon heating, the polynuclear cations in the interlayer space of the LAS turn into metal oxides. These oxides serve as pillars keeping the silicate layers at a certain distance from one another [22].

The degree of dispersion and the coordination environment of iron depend strongly on the origin of the iron cation introduced into the interlayer space. If the iron ions are introduced as the polyhydroxo complex $Fe_x(OH)_y^{n+}$, then the isolated oxide phase Fe_2O_3 will form (Fig. 1). A high degree of dispersion of the metal in the matrix is attained by introducing iron ions as the polynuclear cation $[FeO_4Al_{12}(OH)_{24}(H_2O)_{12}]^{7+}$ [10].

The formation of the polynuclear cation $[FeO_4Al_{12}(OH)_{24}(H_2O)_{12}]^{7+}$ depends strongly on the $OH^-/(Al^{3+} + Fe^{3+})$ and Al^{3+}/Fe^{3+} molar ratios, as is clearly demonstrated by ^{27}Al NMR data (Fig. 4a). The spectrum of an aqueous solution with $Al^{3+}/Fe^{3+} = 10 : 1$ and $OH^-/(Al^{3+} + Fe^{3+}) = 2.4 : 1$ shows two signals with chemical shifts of 63.15 and 0.16 ppm, which are due to the tetrahedrally coordinated aluminunm ions in the polynuclear cation [23] and to $[Al(H_2O)_6]^{3+}$ monomers [24], respectively. Raising the iron content of the system or decreasing the pH of the solution causes a decrease in the intensity of the signal at 63.15 ppm (Fig. 4a, spectra *1–4*). This can be explained by the decomposition of the polynuclear cation into $[Al(H_2O)_6]^{3+}$ and $[Fe_3(OH)_4]^{5+}$. Another important parameter is the synthesis time of the polynuclear cation. Extending the duration of the process shifts the equilibrium toward the formation of the mixed polynuclear cation (Fig. 4a, spectra *4*, *5*). Thus, by varying one of these parameters at the modifying solution preparation stage, it is possible to control the textural properties of the resulting material. It follows from Table 2 that the specific surface area and pore diameter of $Al_{13-x}Fe_x$-LAS decrease as the Al^{3+}/Fe^{3+} ratio is decreased from 12 : 1 to 1 : 1. The textural properties of

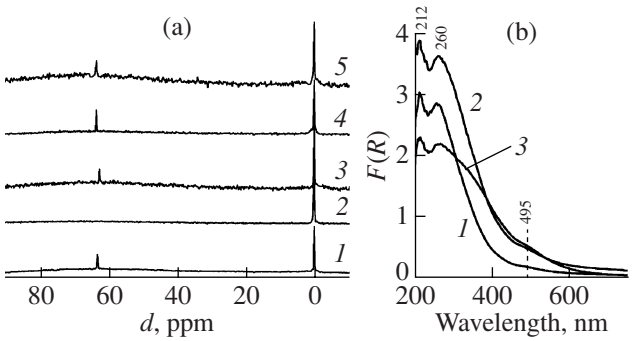

Fig. 4. (a) ^{27}Al NMR spectra of solutions prepared at $OH^-/(Al^{3+} + Fe^{3+})$ = (*1*) 2.0 : 1 and (*2–5*) 2.4 : 1 and Al^{3+}/Fe^{3+} = (*1*, *4*, *5*) 10 : 1, (*2*) 7 : 6, and (*3*) 10 : 3. Spectra *1–4* and spectrum *5* were recorded 7 days and 1 day after solution preparation. (b) Diffuse reflectance spectra of Al_{12}Fe-LAS (M1) samples obtained at $OH^-/(Al^{3+} + Fe^{3+})$ = (*1*) 2.4 : 1 and (*2*, *3*) 2.0 : 1. The polynuclear cation synthesis time is (*1*, *2*) 21 and (*3*) 1 day.

Al_{12}Fe-LAS depend only slightly on the $OH^-/(Al^{3+} + Fe^{3+})$ ratio (Table 3). They depend most strongly on the preparation time of the polynuclear cation $[FeO_4Al_{12}(OH)_{24}(H_2O)_{12}]^{7+}$. As this time is extended from 1 to 7–12 days, the specific surface area of Al_{12}Fe-LAS increases from 125–132 to 209–236 m^2/g (Table 3). A likely cause of this textural change is the strong displacement of the equilibrium toward the formation of the mixed polynuclear cation and, as a consequence, the maximum swelling and separation of the LAS.

CATALYTIC PROPERTIES OF THE MODIFIED LAS'S

Correlation between the Physicochemical and Catalytic Properties of LAS's in Acid Catalysis

Due to the fact that the layered aluminosilicates possess unique textural properties and have rather strong acid sites, they have long been employed as acid catalysts [1, 3–5]. The amount and strength of acid sites are important characteristics of LAS's as catalysts because these parameters usually determine the direction of the reaction and the catalytic activity of the system. Unfortunately, most studies deal with the dependence of catalytic activity on the total acidity of the LAS, not the amount of acid sites of a particular type. Using acetone condensation and methanol addition to propylene oxide, we made an attempt to evaluate the effect of the amount of Lewis acid sites on the catalytic activity of the LAS.

The study of the acid catalytic properties of LAS's in acetone condensation into mesityl oxide (Table 1) demonstrated that the activity of the LAS's increases with an increasing amount and strength of acid sites. For example, this takes place as the LAS calcination temperature is raised. It is rather difficult to establish a

Table 3. Influence of preparation conditions on the catalytic properties of $Al_{12}Fe$-LAS on its catalytic properties in phenol oxidation with hydrogen peroxide

$OH^-/(Al^{3+} + Fe^{3+})$	Sample synthesis time, day	Textural characteristics			[Fe], mg/g	Reaction time, min	PhOH conversion, %	Δ_{Fe}, wt %
		S_{BET}, m^2/g	S_μ, m^2/g	D_{por}, Å				
2.0	1	125	29	71	16 ± 1	40	50	14 ± 2
						155	100	
	21	236	113	72	16 ± 1	90	50	<0.01
						130	100	
2.4	1	132	30	71	15 ± 1	26	50	6 ± 1
						100	100	
	7	219	101	69	17 ± 1	25	50	<0.01
						95	100	
	12	209	96	71	17 ± 2	22	50	<0.01
						90	100	
	21	215	106	72	17 ± 1	22	50	<0.01
						90	100	

Note: Al/Fe = 10 : 1. The samples were calcined at 500°C prior to the reaction. Reaction conditions: [PhOH] = 1 mmol/l; $[H_2O_2]$ = 14 mmol/l; amount of catalyst, 1 g/l; pH 6.2; T = 50°C.

correlation between the origin of the introduced cation and the catalytic activity. However, the Al_{13}-LAS and H-LAS systems, which have sites with $H_0 = -5.6$ and contain the same amount of acid sites with $H_0 = +4.8$ as the Na-LAS system, are more active than the latter. At the same time, although the Al_{13}-LAS and H-LAS system have equal amounts of acid sites with $H_0 = -5.6$, the former is ~2 times more active than the latter (Table 1). This is likely due to the fact that these systems contain different quantities of Lewis acid sites (Table 1). The acetone condensation reaction includes an equilibrium keto-enol rearrangement step and a slow reaction between the enol and a protonated acetone molecule, yielding diacetone alcohol and mesityl oxide [25]:

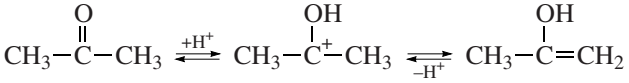

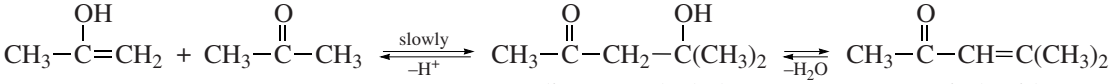

diacetone alcohol mesityl oxide

In the presence of an LAS, this reaction should be viewed as heterogeneous. Its initial step is rapid acetone adsorption yielding the enol form of acetone. This is followed by the polarization of the OH group via its interaction with a Lewis site [26]:

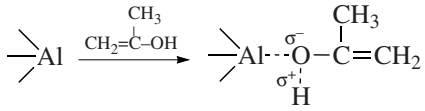

If this is the case, it can be assumed that raising the amount of Lewis sites will speed up the slow step through the polarization of the enolic OH groups and thereby increase the reaction rate.

A glowing example of the effect of the ratio of Lewis and Brønsted acid sites on reaction selectivity is provided by methanol addition to propylene oxide [12]:

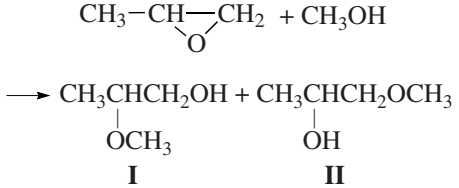

I **II**

Depending on the catalyst, the reaction between propylene oxide and methanol yields either primary or secondary ethers [27]. In the presence of basic catalysts, the main product is 1-methoxypropanol-2 (**II**). In the presence of an acid, the dominant product is 2-methoxypropanol-1 (**I**). Studies of the catalytic activity of LAS's in this reaction demonstrated that the propylene oxide conversion and the product ratio depend on the strength and nature of the acid sites of the LAS (Fig. 5) [12]. The highest activity is shown by the systems containing a large quantity of strong acid sites. The higher activity and selectivity of the Al_{13}-LAS system as compared to the H-LAS system can be explained by the fact that the former has more Lewis sites (Table 1). It is likely that the interaction between a Lewis site and the oxygen bridge of a propylene oxide molecule substantially weakens the C–O bond at which the addition of an alcohol molecule takes place. Note that Al_{13}-LAS and H-LAS far exceed the zeolite catalyst HZSM-5 and bentonite clay in activity and selectivity (Fig. 5).

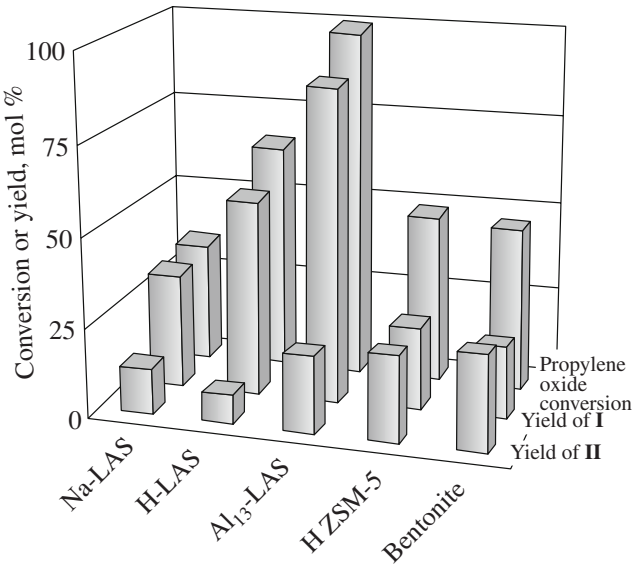

Fig. 5. Methanol addition to propylene oxide in the presence of various acidic catalytic systems ($MeOH/C_3H_7O$ = 10 : 1 mol/mol, 3 wt % catalyst, T = 60°C, reaction time of 6 h).

Influence of the Textural Characteristics of LAS's on Their Catalytic Properties in Oxidation Catalysis

In the last 20–30 years, considerable attention has been given to the problem of removing phenol, one of the most toxic and persistent organic substances, from wastewater. Systems based on iron ions and an LAS can effectively speed up phenol oxidation with hydrogen peroxide into CO_2 and H_2O. However, many of these systems have serious drawbacks, including the following: (1) acids, such as sulfuric and nitric (pH 2–5), must be present; (2) fairly large amounts (>1 wt %) of catalysts must be used; (3) large amounts of the active component are washed out of the catalyst into the solution. The known synthesis methods (see above) afford highly porous LAS's containing a finely dispersed metal. However, there are many questions concerning the correlation between the synthetic methods and the textural and catalytic properties of the resulting catalysts. As is clear from Table 2, the pillaring of Na-LAS by introducing iron ions as $[FeO_4Al_{12}(OH)_{24}(H_2O)_{12}]^{7+}$ into its interlayer space (method M1) yields a catalyst with good technological parameters, namely, a high resistance to iron washout and a high catalytic activity [10]. The systems Al_{12}Fe-LAS (M2) and Al_{12}Fe-LAS (M1) are similar to Na-LAS (M1) in catalytic activity (Table 2, samples 3, 5), but the Al_{12}Fe-LAS (M2) system is less resistant to metal washout from its matrix and, as a consequence, is much less active when reused. The higher activity of Fe-LAS (M3) as compared to Al_{12}Fe-LAS (M1) is also explained in terms of iron ion washout (Table 2, samples 3, 7).

Note the effect of the counterion introduced into the interlayer space of Na-LAS together with iron ions. As can be seen from Table 2, the Fe-LAS(OH) system is more active than the Fe-LAS(Cl) system. This is most likely due to the difference between the textural properties of these systems (Table 2). The pillaring of LAS's with $Fe_x(OH)_y^{n+}$ complexes results in an increase in the specific surface area from 113 to 136 m^2/g, a decrease in the pore volume from 0.28 to 0.27 cm^3/g, an increase in the interlayer spacing from 11 to 14 Å, and a decrease in the pore diameter from 97 to 76 Å. The introduction of $FeCl_3$ does not cause any increase in the interlayer spacing in the sample (10 Å). At the same time, the specific surface area increases to 125 m^2/g; the pore volume, to 0.32 cm^3/g; and the mean pore diameter, to 103 Å. This material (Table 2, sample 8) has large pores and no micropores. Most of the iron of this material is on the surface, and this is why it is very prone to washout [10]. As was discussed above, the textural properties of the modified LAS's can be regulated by varying the $OH^-/(Al^{3+} + Fe^{3+})$ and Al^{3+}/Fe^{3+} molar ratios while synthesizing the polynuclear cation $[FeO_4Al_{12}(OH)_{24}(H_2O)_{12}]^{7+}$. The systems obtained at Al^{3+}/Fe^{3+} = 10 : 1 are the most active and the most stable. Reducing this ratio to 7 : 6 results in the formation of the isolated oxide phase Fe_2O_3 and, accordingly, in a decrease in the stability and activity of the catalyst (Table 2, samples 3, 4). It is noteworthy that the Al_{12}Fe-LAS (M1) system prepared at $OH^-/(Al^{3+} + Fe^{3+})$ = 2.4 : 1 is catalytically more active than the same system prepared at $OH^-/(Al^{3+} + Fe^{3+})$ = 2.0 : 1 (Table 3). The lower activity of the latter is likely due to the presence of a finely dispersed Fe_2O_3 phase. The diffuse reflectance spectrum of the sample prepared at $OH^-/(Al^{3+} + Fe^{3+})$ = 2.0 : 1 shows a band at 495 nm (Fig. 4b), which is characteristic of oligomeric Fe_2O_3 particles. As was mentioned above, a high degree of dispersion of the metal

in the matrix is achieved when the iron ions are introduced as the polynuclear cation $[FeO_4Al_{12}(OH)_{24}(H_2O)_{12}]^{7+}$. The conditions under which this cation was synthesized, namely, the $OH^-/(Al^{3+} + Fe^{3+})$ ratio and particularly the synthesis time have a strong effect on the properties of the resulting material. Extending the cation synthesis time is favorable for the stability and activity of Al_{12}Fe-LAS (M1) (Table 3). This is likely due to changes both in the texture of the material and in the physical state of the iron ions in the matrix, as is suggested by diffuse reflectance data (Fig. 4b, spectra *2*, *3*).

Thus, the catalytic activity and stability of LAS-based systems in acid-catalyzed and oxidation reactions depend on the modification method and conditions and on the origin of the cation introduced into the interlayer space of the LAS.

ACKNOWLEDGMENTS

This study was supported by the Russian Foundation for Basic Research, grant nos. 06-08-01064 and 07-03-90100.

REFERENCES

1. Gil, A. and Gandia, L.S., *Catal. Res. Sci. Eng.*, 2000, vol. 42, p. 145.
2. De Stefanis, A. and Tomlinson, A.A.G., *Catal. Today*, 2006, vol. 114, p. 126.
3. Sels, B.F., de Vos, D.E., and Jacobs, P.A., *Catal. Rev. Sci. Eng.*, 2001, vol. 43, p. 443.
4. Cavani, F., Trifiro, F., and Vaccari, A., *Catal. Today*, 1991, vol. 11, p. 173.
5. Clearfield, A., in *Advanced Catalysts and Nanostructured Materials*, New York: Academic, 1996, p. 345.
6. Rozengart, M.I., V'yunova, G.M., and Isagulyants, G.V., *Usp. Khim.*, 1988, vol. 57, p. 204.
7. Tarasevich, Yu.I., *Stroenie i khimiya poverkhnosti sloistykh silikatov* (Structure and Surface Chemistry of Stratified Silicates), Kiev: Naukova Dumka, 1988.
8. Khankhasaeva, S.Ts., Badmaeva, S.V., Dashinamzhilova, E.Ts., Timofeeva, M.N., Burgina, E.B., Budneva, A.A., and Paukshtis, E.A., *Kinet. Katal.*, 2004, vol. 45, no. 5, p. 708 [*Kinet. Catal.* (Engl. Transl.), vol. 45, no. 5, p. 708].
9. Shchapova, M.A., Khankhasaeva, S.Ts., Ryazantsev, A.A., Batoeva, A.A., and Badmaeva, S.V., *Khim. Interes. Ust. Razv.*, 2002, vol. 10, p. 375.
10. Timofeeva, M.N., Khankhasaeva, S.C., Badmaeva, S.V., Chuvilin, A.L., and Burgina, E.B., Ayupov A.B., Panchenko V.N., Kulikova A.V., *Appl. Catal., B*, 2005, vol. 59, p. 243.
11. Khankhasaeva, S.Ts., Bryzgalova, L.V., Dashinamzhilova, E.Ts., and Ryazantsev, A.A., *Chem. Sustainable Dev.*, 2000, vol. 12, p. 713.
12. Timofeeva, M.N., Mikhalin, N.V., Budneva, A.A., Khankhasaeva, S.Ts., Badmaeva, S.V., and Ryazantcev, A.A., *Acta Mineral. Petrogr. Abstr. Ser. Szeged*, 2004, vol. 4, p. 105.
13. Khankhasaeva, S.Ts., Bryzgalova, L.V., and Dashinamzhilova, E.Ts., *Ekol. Prom–st. Rossii*, 2003, no. 12, p. 37.
14. RF Patent 2 256 498, 2005.
15. Narkynan, S. and Deshpande, K., *Appl. Catal., A*, 2000, vol. 143, p. 17.
16. Prinetto, F., Tichit, D., Teissier, R., and Coq, B., *Catal. Today*, 2000, vol. 55, p. 103.
17. Tarasevich, Yu.I., Ovcharenko, F.D., and Matyash, I.V., *Dokl. Akad. Nauk SSSR*, 1964, vol. 156, p. 926.
18. Godovanaya, O.N. and Tarasevich, Yu.I., *Ukr. Khim. Zh.*, 1976, vol. 42, p. 823.
19. Paukshtis, E.A., *Infrakrasnaya spektroskopiya v geterogennom kislotno-osnovnom katalize* (Infrared Spectroscopy in Heterogeneous Acid Catalysis), Novosibirsk: Nauka, 1992.
20. Yamanaka, S. and Hattori, M., *Catal. Today*, 1988, vol. 2, p. 2610.
21. Lenarda, M. and Ganzrel, R., *J. Mol. Catal.*, 1994, vol. 92, p. 139.
22. Pinnavaia, T.J., Tzou Ming-Shin, Landau, S.D., and Raythatha, R.H., *J. Mol. Catal.*, 1984, vol. 27, p. 195.
23. Palinko, I., Molnar, A., Nage, J.B., Bertrand, J.C., Lazar, K., Valyon, J., and Kirisi, I., *J. Chem. Soc., Faraday Trans.*, 1997, vol. 93, p. 1591.
24. Schutz, A., Stone, W.E.E., Pongelet, G., and Fripiat, J., *Clays Clay Miner.*, 1987, vol. 35, p. 251.
25. Olah, G.A. and Wai, M.I., *New J. Chem.*, 1988, vol. 12, p. 299.
26. Davydov, A., *Molecular Spectroscopy of Oxide Catalyst Surfaces*, Sheppard N.T., Ed., London: Willey, 2003, p. 668.
27. Malinovskii, M.S., *Okisi olefinov i ikh proizvodnye* (Olefin Oxides and Their Derivatives), Moscow: Goskhimizdat, 1961.